Tellus (1999), 51B, 511–530
Printed in UK – all rights reserved

TELLUS
ISSN 0280–6495

Comparison of methods to determine the anthropogenic CO_2 invasion into the Atlantic Ocean

By R. WANNINKHOF[1,*], S. C. DONEY[2], T.-H. PENG[1], J. L. BULLISTER[3], K. LEE[1,4] and R. A. FEELY[3], [1]*NOAA Atlantic Oceanographic and Meteorological Laboratory, Miami, FL33149, USA;* [2]*National Center for Atmospheric Research, Boulder, CO 80307, USA;* [3]*NOAA Pacific Marine and Environmental Laboratory, Seattle, WA 98115, USA;* [4]*Cooperative Institute for Marine and Atmospheric Sciences, University of Miami, Miami, FL33149, USA*

(Manuscript received 27 November 1997; in final form 26 October 1998)

ABSTRACT

A comparison of different methods for estimating the anthropogenic CO_2 burden in the Atlantic Ocean is performed using referenced, high quality total dissolved inorganic carbon (DIC) data. The dataset is from two cruises through the center of the basin between 62°N and 43°S in 1991 and 1993. The specific anthropogenic input is determined utilizing empirical procedures as described in Gruber et al. (1996) and Chen and Millero (1979) to correct for remineralization and to estimate preanthropogenic endmembers. These estimates are compared with output of the Princeton ocean biogeochemical model and the NCAR ocean model. The results show that the specific inventories of anthropogenic carbon agree to within 20% but with different storage and uptake patterns. The empirical estimates differ because of assumptions about mixing and winter outcrop endmembers. The same remineralization quotients (Redfield ratios) were used for each method. Varying these constants within the range of literature values causes changes in specific inventories of similar magnitude as the differences observed with different methodologies. Comparison of anthropogenic CO_2 uptake and chlorofluorocarbon ages suggests that the anthropogenic CO_2 penetration in the North Atlantic is too shallow following the procedure according to Gruber et al. (1996), and too deep using those of Chen and Millero (1979). The results support these previous observations in that the uptake of CO_2 in the North Atlantic is disproportionate to its surface area. This is caused by a combination of deep water formation and deep winter mixed layers.

1. Introduction

Atmospheric CO_2 levels have increased from approximately 280 ppm in pre-industrial times (1750) to 359 ppm in 1993 primarily due to release of anthropogenic CO_2. The rate of release has increased steadily with half the increase occurring in the past 30 years. Oceanic uptake of CO_2 has a strong moderating influence on atmospheric increases. The ocean has taken up one third to one half of the anthropogenic carbon released to the atmosphere to date. This quantification is not exact, and improved knowledge of oceanic inventories will lead to better predictive capacity of future atmospheric CO_2 levels under different fossil fuel release scenarios. The geographic locations of anthropogenic CO_2 storage are important for understanding the pathways and mechanisms of anthropogenic uptake and transport, and the possible changes in uptake in response to climate and global change.

* Corresponding author. NOAA Atlantic Oceanographic and Meteorological Laboratory, 4301 Rickenbacker Causeway, Miami, FL 33149, USA.
E-mail: Wanninkhof@aoml.noaa.gov

The Atlantic Ocean has long been thought to be a major sink of CO_2 (Takahashi et al., 1995). Because of the large scale meridional overturning cell ("conveyer belt"), much of the CO_2 taken up enters the deep ocean and is sequestered on centennial time scales. Several basin wide estimates of anthropogenic CO_2 (DIC_{anthro}) uptake in the North Atlantic have been performed to date (Chen, 1982; Gruber et al., 1996), but they have mainly relied on data obtained from the GEOSECS and TTO cruises that took place 15 to 30 years ago. The uncertainty in the total dissolved inorganic carbon (DIC) data for these cruises is about five times larger than current measurements, which are accurate to 1 to 2 μmol kg^{-1} based on calibration with certified reference materials (CRM).

Several different methods of determining the oceanic anthropogenic inventories have been developed in the past. The anthropogenic CO_2 signal is relatively small, compared with the natural DIC spatial variations, and the key to any such method is how to separate out the natural biological and physical patterns in DIC. Brewer (1978) and Chen and Millero (1979), henceforth referred to as B-78 and CM-79, respectively, proposed methods based on subtracting the soft tissue remineralization and the calcium carbonate dissolution components of the DIC by utilizing changes in oxygen and alkalinity (*T*Alk) with depth, or along isopycnals, together with the remineralization quotient (Redfield ratio) between carbon and oxygen. The results of this exercise are critically dependent on the remineralization quotient used. Assumptions about surface alkalinity and DIC values in wintertime outcrop areas have a significant influence on the inventory estimates as well. Mixing of water masses is accounted for in a simplistic manner by normalizing the *T*Alk and DIC to constant salinity. In these analyses it is assumed that the oldest waters in the interior do not contain any DIC_{anthro} at the time of measurement. The initial work by B-79 and CM-79 had as major objective to estimate preanthropogenic atmospheric partial pressure of CO_2 (pCO_{2a}) assuming that the surface ocean was at equilibrium with the atmosphere.

Although, what now appear to be reasonable estimates of preanthropogenic pCO_{2a} were obtained compared to historical atmospheric CO_2 records from CO_2 in bubbles of ice cores (Neftel et al., 1985), the uncertainty in the pCO_{2a} estimate was approximately 10 to 15 μatm. Subsequent work by Chen (1993) extended the analysis from the Atlantic thermocline to whole ocean inventories of DIC_{anthro}. Recently, improvements in this type of inventory estimate have been proposed by Gruber et al. (1996) (GSS-96) who employed better methods to estimate mixing of water masses with different preformed concentrations. They also utilized the transient tracer pair ^3H–^3He to estimate the DIC_{anthro} on shallow isopycnals that are completely ventilated in the past 40 years, and they accounted for the pCO_2 disequilibrium between ocean and atmosphere at the outcrops.

An independent approach to the empirical inventory calculations is to utilize ocean circulation models. Box models calibrated using observations of bomb ^{14}C penetration gave the initial estimates of global DIC_{anthro} uptake by the ocean (Oescher et al., 1975). More sophisticated general circulation models have subsequently been used to estimate uptake for individual ocean basins or ocean sections. In our comparison we utilize the NCAR and the Princeton versions of the ocean biogeochemistry model (OBM), both of which are derived originally from the Cox and Bryan model (Bryan and Lewis, 1979).

The objective of our work is to perform a critical comparison among inventory estimates along a meridional section in the Atlantic Ocean from 62°N to 43°S. The section under investigation was occupied as part of the Ocean-Atmosphere Carbon Exchange Study (OACES) of the National Oceanic and Atmospheric Administration (NOAA). The southern segment from 5°N to 43°S along nominally 25/32°W (Fig. 1) was occupied in the austral winter (July) of 1991. The northern section from 5°S to 62°N along 20/25°W was performed in July/August of 1993. To estimate DIC and *T*Alk outcrop values at high latitude, we used data from the Transient Tracers in the Ocean study, TTO (TTO, 1986) and the South Atlantic Ventilation experiment (SAVE/HYDROS) (Takahashi, pers. com.; SAVE (1992)). The carbon inventory obtained along the cruise track is not extrapolated basinwide since there are likely appreciable East–West gradients with the Western Basin containing more DIC_{anthro} due to rapid transport within the deep western boundary current (Chen, 1982; Gruber et al., 1996; Körtzinger et al. 1998). The basin wide inventory can be

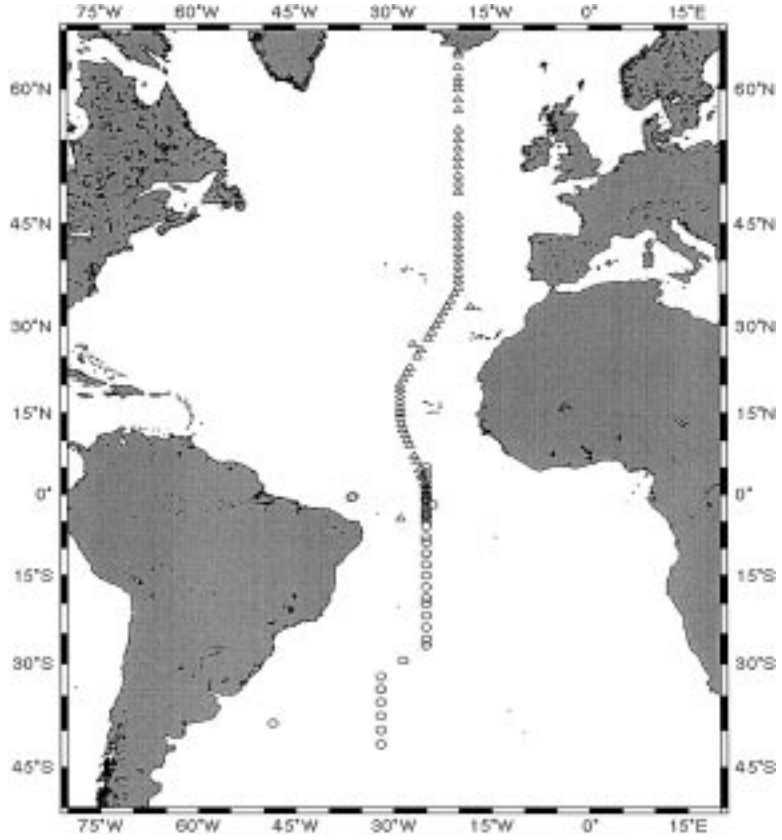

Fig. 1. Data for the analysis were obtained from the observations at the stations depicted. The South Atlantic section (circles) was occupied in July 1991 (S. Atl-91), and the northern leg (triangles) was occupied in July 1993 (N. Atl-93) as part of the NOAA/OACES program.

performed with high accuracy after completion of the CO_2 survey sponsored by the US Department of Energy and NOAA in 1998.

We will first describe the dataset as it pertains to our analysis with emphasis on accuracy, precision, and internal consistency of the relevant data between the two cruises. The methodology for calculation of DIC_{anthro} and the results from the different estimates is given in Section 3. The agreement and differences between the methods is detailed by comparing remineralization quotients and correspondence with chloro-fluoro carbon ages, (τ_{CFC}) in the last part of the paper.

2. Description of field data

Since the DIC_{anthro} is at most 3% of the DIC in the surface and rapidly decreases with depth, accurate measurements of DIC, the fugacity of CO_2 (fCO_2) or total alkalinity (TAlk), oxygen (O_2), temperature (T), and salinity (S) are necessary. The fCO_2 is the pCO_2 corrected for a small non-ideality of CO_2 in air ($fCO_2 \approx 0.996\ pCO_2$). Furthermore, nitrate or phosphate measurements are needed for estimating preformed endmember values. The analytical methods for the datasets are reported in Castle et al. (1998), Forde et al. (1994), and Lee et al. (1997). Changes in alkalinity are used to correct for increases in DIC due to the calcium carbonate dissolution during transport of water into the interior. Here it is calculated from fCO_2 and DIC rather than using the TAlk observations from the cruises. The quality of the TAlk data during the 1991 cruise in the South Atlantic, henceforth called S. Atl-91, is not as good as subsequent measurements during the North

Atlantic cruise in 1993 (N. Atl-93). Best agreement between measured alkalinity and calculated alkalinity from fCO_2 and DIC is obtained using the constants of Mehrbach et al. (1973) as determined with the program of Lewis and Wallace (1998). For the S. Atl-91 dataset the difference between measured and calculated TAlk from DIC and fCO_2 is 1.4 ± 10.3 μEq kg^{-1} ($n = 223$) while for the N. Atl-93 dataset the offset is -3.8 ± 4.8 μEq kg^{-1} ($n = 1557$).

For both cruises DIC measurements were performed using coulometers with a SOMMA (single operator multi-parameter metabolic analyzer) inlet system (Johnson et al., 1993). Certified reference materials (CRM Batch #16) were provided by Dr. Dickson of SIO. The analyses for each instrument were corrected to the cruise average CRM values for the instrument by applying a constant offset. For each cruise the corrections were less than 2 μmol kg^{-1} while the standard deviations of all CRMs analyzed during the cruises were less than 1.5 μmol kg^{-1}. DIC measurements from the N. Atl-93 and S. Atl-91 cruises were compared in the region of overlap between 5°S and 5°N using deep water where calibration offsets would be most apparent. No offset in DIC was detected between the N. Atl-93 and S. Atl-91 data. $fCO_2(20)$ was measured by equilibration of a headspace with a water sample at constant temperature (20.00°C) and detection with a non-dispersive infrared detector as detailed in Chen et al. (1995). Precision of the $fCO_2(20)$ measurements based on 31 replicate samples taken at different depths was 0.2% for the N. Atl-93 cruise, while the precision of the S. Atl-91 cruise was estimated at 0.3%. Again no detectable bias was observed in the deep waters in the region of overlap for the two cruises. Oxygen values had a precision of 1 μmol kg^{-1} for both cruises. The deep water O_2 data from the S. Atl-91 cruise showed good correspondence with the SAVE 5/HYDROS 4 cruises along similar cruise tracks.

However, the N. Atl-93 O_2 data had a significant offset compared to the Oceanus-202 cruise along the same track (Tsuchiya et al., 1992). This offset is apparent in the whole water column but can be best quantified in the deep water where a difference of 7.5 ± 1 μmol kg^{-1} was observed with the N. Atl-93 data being lower. We assume that the N. Atl-93 data are biased because the surface water values are at or slightly below saturation rather than slightly supersaturated as typical in the surface ocean. A likely cause for the offset is a bias in the thiosulfate standard reagent. To account for this discrepancy a value of 7.5 μmol kg^{-1} was added to all N. Atl-93 O_2 values.

3. Determination of anthropogenic CO_2

The method of determining the DIC_{anthro} by the empirical method is described in detail elsewhere (Chen and Millero, 1979; Chen, 1982; Chen et al., 1990; Gruber et al., 1996). Here we will only reiterate the important points and emphasize the differences between the method of CM-79 and the recent method developed by GSS-96. Both methods have the same basic underlying assumption that the DIC_{anthro} signal can be determined by differences in preformed carbon along isopycnals, or with depth, by subtracting the remineralization and carbonate dissolution component of the observed DIC. The fundamental equation for both methods is the same in that:

$$\begin{aligned} DIC_{anthro} &= \Delta DIC - 0.5[\Delta T\text{Alk} + R_{N:O}(\Delta AOU)] \\ &\quad + R_{C:O}(\Delta AOU), \\ \Delta X &= X_x - X_0, \end{aligned} \tag{1}$$

where DIC_{anthro} is the anthropogenic DIC component, AOU is the apparent oxygen utilization, and $R_{N:O}$ and $R_{C:O}$ are the remineralization quotients between NO_3 and O_2, and DIC and O_2, respectively. ΔX is the difference in the in situ measurements, X_x and the preformed preanthropogenic value at the outcrop, X_0, where X is DIC, TAlk, or AOU. The $R_{N:O}$ (ΔAOU) is the "nitrate contribution" to alkalinity due to soft tissue remineralization (Brewer et al., 1975). A summary of symbols can also be found in Section 7.

There are several major sources of uncertainty in the calculation of DIC_{anthro} from (1) including uncertainty in remineralization quotients and preformed concentrations in the outcrop region. The remineralization quotients, R, are not well known and possibly vary with depth (Minster and Boulahdid, 1987). Anderson and Sarmiento (1994) assign the following ratios and uncertainties to the remineralization quotients: $P:N:C:-O = 1:16 \pm 1:117 \pm 14:170 \pm 10$ based on a thorough isopycnal analysis of the world's oceans. In their

work they excluded the North Atlantic where mixing of different water masses confounded their analysis. If we assume these are typical uncertainties for remineralization quotients and propagate the error in C : –O, the uncertainty in $R_{C:O}$ is 12%. This has a significant influence on the calculated DIC_{anthro}. Fig. 2 shows the fractional error caused by this uncertainty relative to the observed DIC_{anthro} level for the two empirical methods described below. The rapidly increasing fractional error is caused by a combination of increasing ΔAOU and decreasing DIC_{anthro} for older waters.

The preanthropogenic preformed values in the wintertime outcrop have to be estimated and interpolated against temperature, or other quasi-conservative parameter. It is assumed that the alkalinity has not changed due to anthropogenic perturbation. In CM-79, salinity normalized alkalinity is regressed against temperature in the surface mixed layer such that $NTAlk_0$ can be estimated for each sample. The preanthropogenic (AOU_0) and current apparent oxygen utilization are assumed to be 0 at the outcrop. Oxygen concentrations at the surface could differ by several percent either because of supersaturation due to bubble entrainment, or because of undersaturation due to outcropping of undersaturated water and insufficient time for equilibration with the atmosphere. The largest uncertainty in CM-79 arises because of assumptions in determining the ΔDIC term. DIC_0 is not known such that as a first-step DIC_{ot}, the present-day preformed DIC in the wintertime outcrop, is estimated. In CM-79, salinity normalized DIC_{ot} is regressed against temperature at the surface such that DIC_{ot} can be determined for all (subsurface) water samples with knowledge of T.

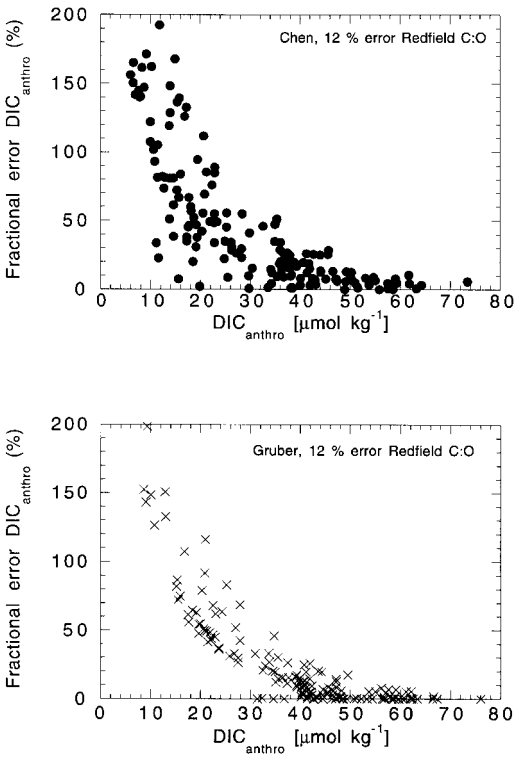

Fig. 2. Fractional error in DIC_{anthro}(%) plotted against DIC_{anthro} assuming a 12% uncertainty in the C : O ratio. (a) DIC_{anthro} calculated following the methods of CM-79; (b) DIC_{anthro} calculated following the methods of GSS-96.

The shortcomings of the CM-79 method have been clearly described in Broecker et al. (1985) and have been addressed, in part, in GSS-96. While CM-79 accounts for mixing processes by normalizing to salinity, this does not fully account for unique temperature dependences of $NTAlk_0$ and $NDIC_{ot}$ for different outcrop regions. This is particularly an important issue in the Atlantic where the waters from northern origin mix with waters from the south that have very different preformed quantities. GSS-96 estimates preformed alkalinity for the entire Atlantic by creating a multiple linear regression of alkalinity against salinity and the quantity "PO" (Broecker, 1974). This relationship is thought to be valid for all outcrops and shows good agreement with sparse wintertime data as well.

The second significant improvement of GSS-96 over CM-79 is the attempt to account for DIC_{anthro} in the upper thermocline where isopycnals have been ventilated during the period of anthropogenic change. This is done by determining the water mass age using the helium–tritium (^3H–^3He) dating technique. However, ^3H–^3He ages are not true watermass ages because of mixing (Jenkins, 1988) and tend to underestimate age beyond about 15 years (Doney et al., 1997). This method only yields ages since the large bomb tritium inputs, 30 to 40 years ago at which point half the atmospheric C_{anthro} had already entered the ocean.

3.1. The empirical method according to Chen and Millero (1979)

The first application of the method of CM-79 was to estimate preanthropogenic pCO_{2a} values.

Subsequently, the utility was expanded to estimate DIC_{anthro} in the ocean. For the initial work, the anthropogenic perturbation was set, by definition, at 0 at the surface and decreased with depth. Subsequently, modifications to the approach were made, using the term defined below as $(\Delta NDIC)_{min}$, such that the deep water attain a DIC_{anthro} of 0 and surface waters the showed full anthropogenic burden. Thus, what we describe as the CM-79 method actually includes the refinements as discussed in a later publication (Chen, 1993).

The pertinent calculations for the CM-79 method are as follows:

$$DIC^{cm}_{anthro} = \Delta NDIC^{cm} - 0.5 \times [\Delta NTAlk + R_{N:O}(AOU)] + R_{C:O}AOU, \quad (2)$$

$$\Delta NDIC^{cm} = NDIC - NDIC_{ot} - (\Delta NDIC)_{min} \quad (3)$$

where DIC^{cm}_{anthro} is the anthropogenic component of the measured DIC according to CM-79. $\Delta NTAlk$ is difference in salinity normalized $TAlk$ (= Talk*35/S) between the outcrop and point of measurement. $\Delta NDIC^{cm}$ is difference between the measured salinity normalized DIC and the current day outcrop value, $NDIC_{ot}$, corrected for the minimum value obtained at depth, $(\Delta NDIC)_{min}$. The $(\Delta NDIC)_{min}$ is the lowest value of $(NDIC_c - NDIC_{ot})$ observed at depth, where $NDIC_c = NDIC - 0.5[\Delta NTAlk + R_{N:O}(AOU)] + R_{C:O}$ AOU. This causes a bias if the anthropogenic signal has penetrated to the bottom, as occurs in our section, or if waters are mixtures of endmembers with different characteristic $NDIC_{ot}$ and $NTAlk_0$. Typical values of $(\Delta NDIC)_{min}$ are -50 to -60 μmol kg^{-1}.

For our current exercise, we used the remineralization quotients recommended in Anderson and Sarmiento (1994). Our surface water data do not cover temperatures less than 10°C, so the surface water $NTAlk_0$ algorithms with temperature were obtained from a compilation of data from the N. Atl-93, SAVE, and TTO cruises for the N. Atlantic, and the S. Atl-91 and GEOSECS cruises for the S. Atlantic (Millero et al., 1998).

The $NTAlk_0$ is nearly constant at 2291 ± 4 μEq kg^{-1} for $T > 20$°C. It is fit to:

$$NTAlk_0 = 2291 - 2.69(T - 20) - 0.046(T - 20)^2 \quad (4)$$

for $T < 20$°C in the North Atlantic, and

$$NTAlk_0 = 2291 - 2.52(T - 20) + 0.056(T - 20)^2 \quad (5)$$

for $T < 20$°C in the South Atlantic

The standard deviation is ± 5 μEq kg^{-1} between the fits and the observations. These fits along with N. Atl-93 and S. Atl-91 surface water data (0–40 m) data are shown in Fig. 3a. The algorithms yield a slightly lower alkalinity than observed in our datasets. The average surface water $NTAlk$ for $T > 20$°C for our data is 2295 ± 5 μEq kg^{-1} versus 2291 ± 4 μEq kg^{-1} for the more comprehensive dataset used by Millero et al. (1998). The differences are not statistically significant and have little influence on the DIC_{anthro} calculation since most of the DIC_{anthro} inventory resides in water with $T < 20$°C.

For $NDIC_{ot}$ we chose a relationship for water originating from the southern hemisphere of $NDIC_{ot} = 2227 - 11.5T$ and for water from the northern hemisphere of $NDIC_{ot} = 2143 - 7.58T$. These relationships were obtained by fitting the data from the TTO cruises (TTO, 1986) and METEOR cruises (Chipman et al., 1991) as they include an abundance of samples at $T < 15$°C. No correction was made to account for changes in $NDIC_{ot}$ caused by the different times at which the cruises occurred since the correction would be significantly less than the uncertainty in the relationships. The correspondence of the relationships with our data is reasonable over the common temperature range (Fig. 3b). For the S. Atl-91 data, which only extends to mid-southern latitude, the $\Delta NDIC_{ot}$ (observed–calculated) equals 20 ± 20 μmol kg^{-1}, while for the North Atlantic the difference is 6 ± 9 μmol kg^{-1}.

The empirical relationships to determine $NTAlk_0$ and particularly $NDIC_{ot}$ are critical and can vary significantly depending on the formulation used (Fig. 3c). $NTAlk_0$ establishes the correction for $CaCO_3$ dissolution when water ages and moves into the interior. The $NDIC_{ot}$ are the current preformed values on which the entire anthropogenic inventory is based. The differences in the relationships of $NDIC_{ot}$ versus temperature can be illustrated from the range algorithms for $NDIC_{ot}$ developed for different parts of the

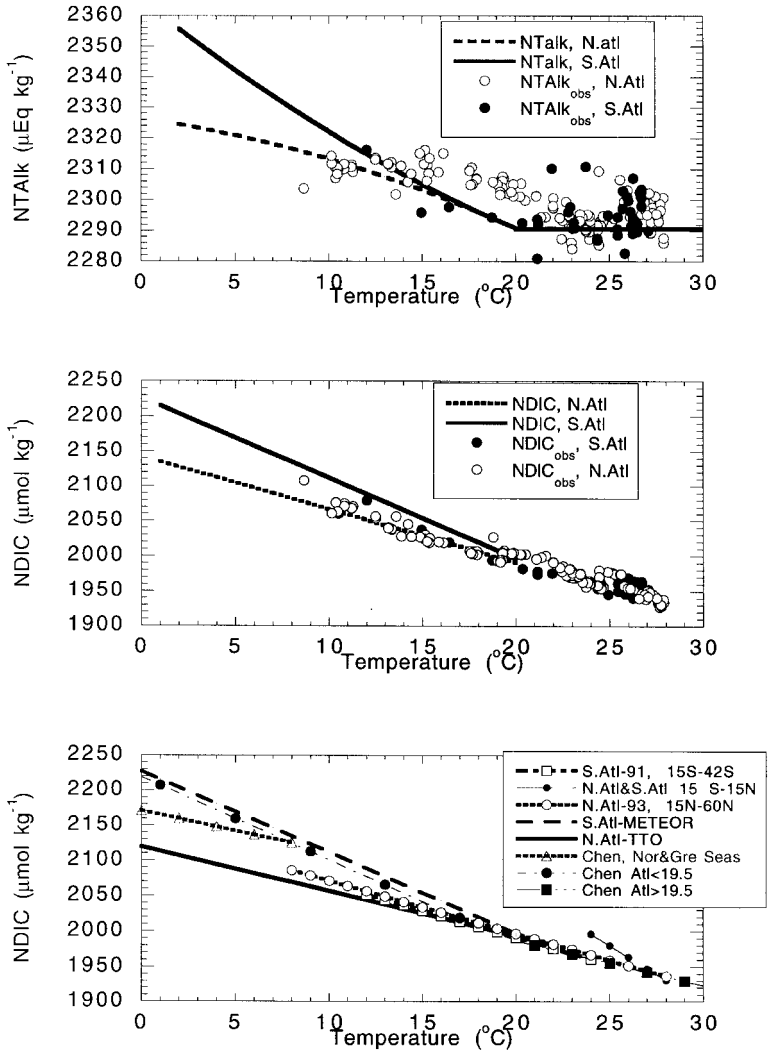

Fig. 3. Relationships between sea surface temperature and salinity normalized ($S = 35$) alkalinity (N*T*Alk), and total dissolved inorganic carbon (NDIC) used in the analysis according to CM-79. The relationships show large differences in northern and southern endmembers for N*T*Alk (a) and NDIC (b). The open circles are the surface observations during N. Atl-93 while the solid circles are those from S. Atl-91. (c) Shows the relationships for different cruises and temperature ranges and locations (Table 1).

Atlantic, and with different datasets. Because the calculated $NDIC_{ot}$ is strongly dependent on T (Table 1), the choice of relationship can alter the total inventories. In particular, since most of the ocean has temperatures less than 10°C, differences in the relationship at low T, where we have little surface water data, will have a large influence on the DIC_{anthro} calculation. Improvements in the $NDIC_{ot}$ relationships can be attained by creating relationships for smaller geographic regions.

The choice of using northern or southern $NTAlk_0$ and $NDIC_{ot}$ endmembers for a particular water parcel will have a significant influence on the results as well. For the thermocline and sub-thermocline waters with temperatures between 20°C and 3°C, we chose 15°N as a division based

Table 1. *Algorithms of $NDIC_{ot}$ versus temperature*

All surface waters S. Atl-91 and N. Atl-93:	$NDIC_{ot}(\pm 9.2) = 2142–7.226T$
(data from OACES S. Atl-91 and N. Atl-93)	
S. Atl-91: 15°S–42°S:	$NDIC_{ot}(\pm 7.8) = 2143–7.596T$
(data from OACES S. Atl-91 and N. Atl-93)	$T = 10–24°C$
S. Atl-91 and N. Atl-93: 15°S–15°N:	$NDIC_{ot}(\pm 9.0) = 2390 - 16.4T$
(data from OACES S. Atl-91 and N. Atl-93)	$T = 24–30°C$
N. Atl-93: 15°N–60°N:	$NDIC_{ot}(\pm 8.2) = 2146 - 7.48T$
(data from OACES S. Atl-91 and N. Atl-93)	$T = 8–25°C$
South Atlantic METEOR (Chipman et al., 1991):	$NDIC_{ot} = 2227 - 11.5T$
	$T = 0–22°C$
TTO N. Atlantic (TTO, 1986):	$NDIC_{ot} = 2143 - 7.58T$
	$T = 0–22°C$
TTO N. Atlantic and N. Atl-93:	$NDIC_{ot} = 2119.7 - 6.3T$
Atlantic and Southern Ocean (Chen, 1982):	$NDIC_{ot} = 2219 - 11.8T,\ T < 19.5$
	$NDIC_{ot} = 2115 - 6.4T,\ T > 19.5$
Greenland and Norwegian Sea (Chen et al., 1990):	$NDIC_{ot} = 2171 - 5.7T$

on the sharp change of salinity along isopycnals. Large tritium and CFC gradients also suggest slow exchange across this boundary (Broecker and Ostlund, 1979; Doney and Bullister, 1992). For deep waters ($T < 3°C$), the equator was chosen as a division based on the predominance of Antarctic waters south west of the Mid Atlantic Ridge and water of northern origin north (east) of the Ridge as indicated by large silica gradients. In reality, there will be a large region with an admixture of waters from northern and southern origin.

Once the relationships of $NDIC_{ot}$ and $NTAlk_0$ have been established, the difference between $NDIC_c$ and $NDIC_{ot}$ is determined. The value will be 0 at the surface and reach a minimum (negative) value at depth, $(\Delta NDIC)_{min}$. Subsequently, this minimum value is subtracted from each $NDIC - NDIC_{ot}$ determination to estimate DIC^{cm}_{anthro}. The deep water values are averaged over 20° latitude bands south of 20°N and this $(\Delta NDIC)_{min}$ is subtracted from all the values above. From 20°N northward, $(\Delta NDIC)_{min}$ between 0° and 20°N is used. The data is subsequently gridded corresponding to the Princeton OBM depth bins for comparison with the model results. Fig. 4a shows the expected features of deep penetration of DIC^{cm}_{anthro} in the thermocline outcropping and intermediate/deep water formation areas. Higher penetration is apparent in the northern latitudes compared to the south. The large DIC^{cm}_{anthro} signal of greater than 50 μmol kg^{-1} in the subpolar North Atlantic with a subsurface maximum corresponds to the recently ventilated Labrador Sea Water. The low values in the top 1000 m subtropical Atlantic cannot readily be explained and could be an artifact of our choice of $NTAlk_0$ and $NDIC_{ot}$. The separation of waters ventilated to the bottom in the north and more isolated southern waters is apparent between 15° and 20°N. A uniform penetration of DIC^{cm}_{anthro} is observed between 10°N and 30°S with a very rapid drop off and barely detectable DIC^{cm}_{anthro} levels below 800 m. Further southward in the subtropics penetration increases to over 1500 m.

A rigorous analysis of uncertainties is difficult because of somewhat subjective choices of preformed values and remineralization quotients. Previously, the uncertainty has been estimated ranging from 15 μmol kg^{-1} (Chen, 1982) to 10 μmol kg^{-1} (Chen, 1993) with the improvement largely because of smaller uncertainties in the analytical precision. We estimate our uncertainty at a similar level as the recent work by Chen. Fig. 5a shows the specific inventory of DIC^{cm}_{anthro}

Fig. 4. Cross sections of DIC_{anthro} for the Atlantic basin following the cruise track shown in Fig. 1 using the methodology of CM-79 (a); the approach of GSS-96 (b); the output from the Princeton OBM (c); and NCAR OBM (d). The data shown in (a) and (b) were gridded in the same bin sizes as the OBM (5° horizontal and 12 depths increasing in size going downward) before contouring. The 0.1 pmol kg^{-1} CFC-11 isopleth (corresponding roughly to a τ_{CFC} of 30–35 years) is shown by the plus symbols.

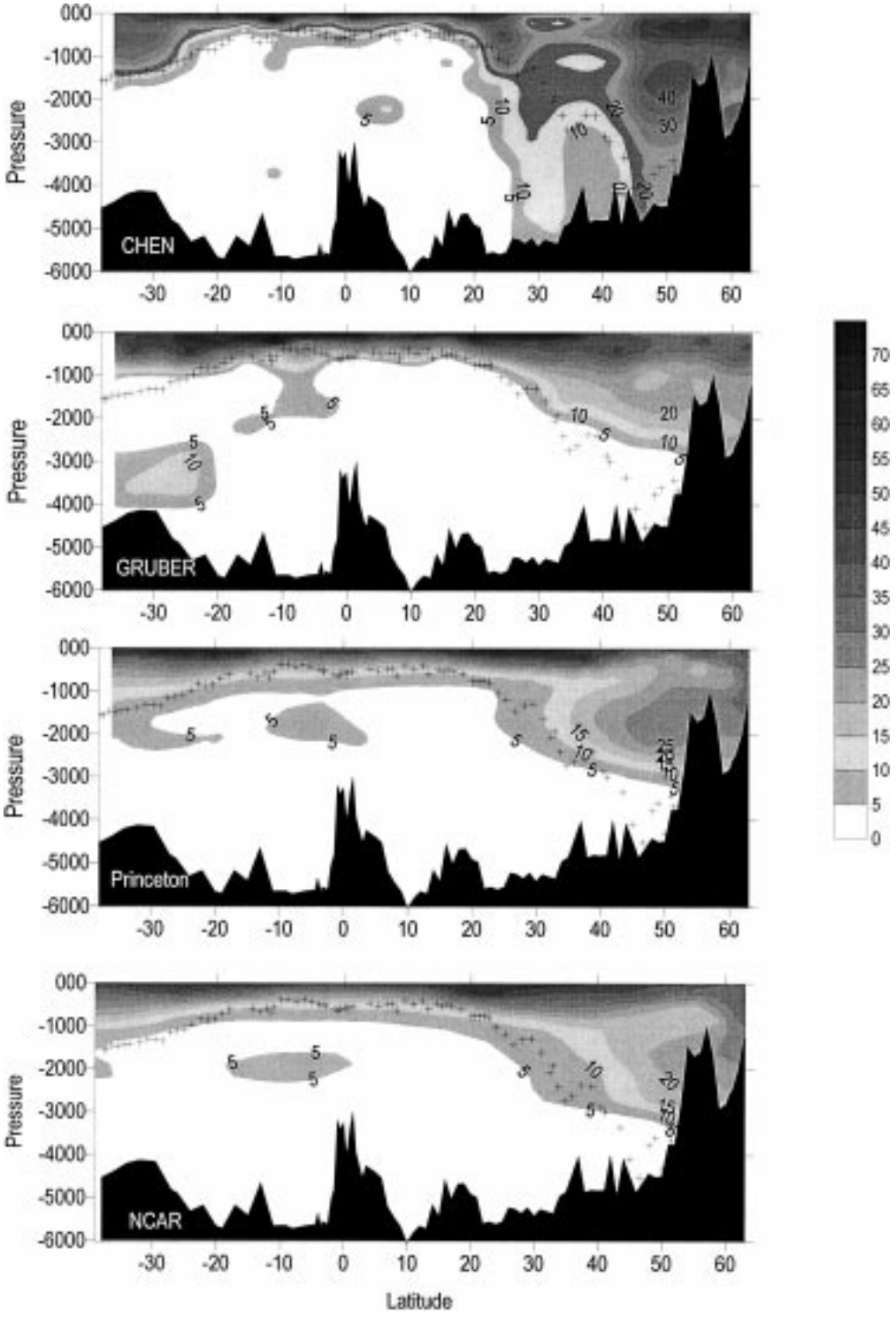
CHEN
GRUBER
Princeton
NCAR
Pressure
Latitude
000
-1000
-2000
-3000
-4000
-5000
-6000
-30
-20
-10
0
10
20
30
40
50
60
70
65
60
55
50
45
40
35
30
25
20
15
10
5
0

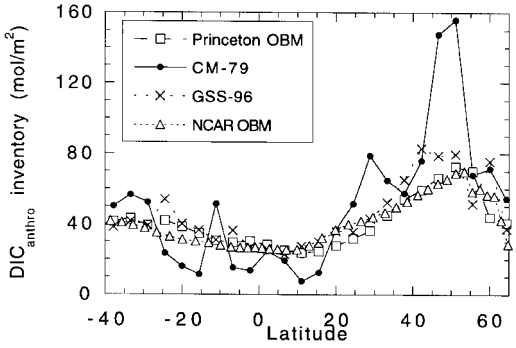

Fig. 5. Specific water column inventories using the methodology of GSS-96 (crosses); CM-79 (solid circles); output from the Princeton OBM (open squares); and NCAR OBM (open triangles).

binned in 5° latitude bands. The specific inventory varies by almost a factor of ten with very high specific inventories in the north, intermediate levels in the south and lower inventories at low latitudes.

3.2. *The empirical method according to Gruber, Sarmiento, and Stocker (1996)*

The analysis according to GSS-96 employs the same general principles as the earlier methods but with some significant improvements. The method employs a quasi-conservative quantity C^*:

$$C^* = \mathrm{DIC} - 0.5(T\mathrm{Alk} + R_{\mathrm{N:O}}\mathrm{O}_2) - R_{\mathrm{C:O}}\mathrm{O}_2 \qquad (6)$$

A similar equation can be set up for C_0^* in which DIC, TAlk, and O_2 are replaced by their preanthropogenic preformed values. The difference is defined as ΔC^*:

$$\Delta C^* = C^* - C_0^* = \Delta\mathrm{DIC}^{\mathrm{G}} - 0.5\Delta T\mathrm{Alk} + (R_{\mathrm{C:O}} - 0.5R_{\mathrm{N:O}})\mathrm{AOU}, \qquad (7)$$

where

$$\Delta\mathrm{DIC}^{\mathrm{G}} = \mathrm{DIC} - \mathrm{DIC}_{\mathrm{eq}}(S, T, T\mathrm{Alk}_0)_{p\mathrm{CO}_{2\mathrm{a}}} = 280.$$

$\Delta\mathrm{DIC}^{\mathrm{G}}$ is the difference in measured DIC and the DIC in equilibrium with a $p\mathrm{CO}_{2\mathrm{a}}$ of 280 µatm at in situ S, T, and preformed alkalinity value, $T\mathrm{Alk}_0$. ΔC^* is similar to the definition of $\mathrm{DIC}_{\mathrm{anthro}}$ outlined above in (1). More precisely ΔC^* is the $\mathrm{DIC}_{\mathrm{anthro}}$ if the surface ocean was in equilibrium with the atmosphere with a $p\mathrm{CO}_{2\mathrm{a}}$ of 280 µatm, discounting any influence of non-linear mixing effects along isopycnals.

From our data in the top 100 m, we determined a relationship for $T\mathrm{Alk}_0$:

$$T\mathrm{Alk}_0 = (278.4 + 57.01\mathrm{S} + 0.0074\mathrm{NO}) \qquad (8)$$
$$r^2 = 0.97, \qquad n = 350,$$

where $\mathrm{NO} = \mathrm{O}_2 + R_{\mathrm{N:O}}\mathrm{NO}_3$ (Broecker, 1974). This result is similar to the calculated $T\mathrm{Alk}_0$ obtained by GSS-96 from older data in the N. Atlantic. The standard deviation between the observed $T\mathrm{Alk}_0$ and predicted $T\mathrm{Alk}_0$ from (8) is 5.2 µEq kg^{-1}. $\mathrm{DIC}_{\mathrm{eq}}$ for our work were calculated from the derived $T\mathrm{Alk}_0$ (8) and $p\mathrm{CO}_{2\mathrm{a}} = 280$ µatm using the dissociation constants of Mehrbach et al. (1973). These resulting $\mathrm{DIC}_{\mathrm{eq}}$ are subsequently linearized as in GSS-96 using a least squares linear fit:

$$\mathrm{DIC}_{\mathrm{eq}} = 2082.787 + 0.782249(T\mathrm{Alk}_0 - 2320) - 5.10296(S - 35) - 8.99668(T - 9)$$
$$r^2 = 1.00, \qquad n = 335 \qquad (9)$$

with a standard deviation between the calculated $\mathrm{DIC}_{\mathrm{eq}}$ and the linearized $\mathrm{DIC}_{\mathrm{eq}}$ of 1.4 µmol kg^{-1}. The temperature, T is in °C.

The $\mathrm{DIC}^{\mathrm{G}}_{\mathrm{anthro}}$ is subsequently calculated, accounting for the air–sea disequilibrium, expressed in terms of DIC (ΔC_{dis}), by two different methods depending if the particular isopycnal in the interior of the Atlantic contains measurable CFCs or not. For isopycnals that are CFC-free in the interior ($\mathrm{CFC} - 11 < 0.005$ pmol kg^{-1}), the disequilibrium, ΔC_{dis} is the ΔC^* of the interior endmember of the particular isopycnal in the interior and $\mathrm{DIC}^{\mathrm{G}}_{\mathrm{anthro}} = \Delta C^* - \Delta C_{\mathrm{dis}}$. For the Atlantic the density surfaces referenced to 2000 dB, σ_2 of greater than 36.85 are CFC-free in the interior. For isopycnals that have measurable CFC-11 on the interior endmember, the disequilibrium is estimated from the CFC age (τ_{CFC}) of the water and the corresponding atmospheric CO_2 level, $p\mathrm{CO}_{2(\tau\mathrm{CFC})}$, for that age:

$$\Delta C_{\mathrm{dis}_t} = \Delta\mathrm{DIC}^{\mathrm{G}}_t - 0.5\Delta\mathrm{N}T\mathrm{Alk} + (R_{\mathrm{C:O}} - 0.5R_{\mathrm{N:O}})\mathrm{AOU}, \qquad (10)$$

where

$$\Delta\mathrm{DIC}^{\mathrm{G}}_t = \mathrm{DIC} - \mathrm{DIC}_{\mathrm{eq}}(S, T, T\mathrm{Alk}_0)_{p\mathrm{CO}_{2(\tau\mathrm{CFC})}}$$
$$\mathrm{DIC}^{\mathrm{G}}_{\mathrm{anthro}} = \Delta C^* - \Delta C_{\mathrm{dis}_t}.$$

The τ_{CFC} is calculated by converting the CFC-11

concentrations in the water to partial pressure (pCFC) at the potential T and S (Doney and Bullister, 1992) and then matching pCFC of the water parcel with the pCFC of the atmosphere for the appropriate year. If the transport into the interior is primarily advective with little mixing between waters with significantly different CFC-11 concentrations, the τ_{CFC} is roughly the age since the water lost contact with the atmosphere.

The general pattern of DIC^{G}_{anthro} as shown in Fig. 4b is similar to DIC^{cm}_{anthro} with deep penetration in the high northern latitude and penetration to about 1000 m in the tropical gyres. The significant signal in the south at 3000–4000 m of 10–15 μmol kg^{-1} corresponds to water from Antarctic origin. The elevated values just south of the equator at 1500 and 3000 m coincides with measurable CFC-11 levels and appear to be associated with the equatorial limb of the Deep Western Boundary Current ventilating the deep water on short time scales (Takahashi et al., 1994; Doney et al., 1997).

The comparison of the computed disequilibrium, ΔC_{dis} with that of GSS-96 shows good correspondence for the isopycnal surfaces down to $\sigma_2 = 36.75$ (Fig. 6). For denser surfaces there is deviation with our study suggesting significantly larger disequilibria. The smaller values in GSS-96 appear more reasonable, but since these dense isopycnals do not outcrop but rather take up CO_2 by deep water formation and mixing processes, the analysis likely is questionable for these levels. These surfaces have only taken up a limited amount of DIC_{anthro} such that it does not influence the overall inventory significantly. The good correspondence at shallow isopycnals between this work and that of GSS-96 is an indication of the good agreement in the independently derived empirical relationships for DIC_{eq}, $TAlk_0$, ΔC_{dis_t} and the good correspondence between the different datasets.

3.3. *The Princeton and NCAR numerical models*

The 3rd estimate of CO_2 uptake is obtained from numerical computer models, the Princeton and NCAR 3-dimensional OBM. The model outputs are dependent on the numerical advection and dispersion schemes, the parameterization of physical and biological processes, and boundary conditions. Due to their complexity, the OBMs are not changeable by the casual user. The general circulation models are powerful to study uptake patterns and to estimate future CO_2 levels in ocean and atmosphere. The steady state salinity, temperature, DIC and TAlk fields differ from the observations because of the inability of the models to form sufficient amount North Atlantic Deep water at the appropriate depth. As a result the model basin is flooded with water of Antarctic origin with significantly higher DIC and TAlk. However, this is not thought to have a large effect on the CO_2 perturbation experiments described below.

The Princeton OBM is run with annual mean climatology and water chemistry, and has 12 unevenly spaced layers in the vertical and a grid size of nominally 4.5° latitude and 4° longitude. Details of the Princeton OBM can be found in Sarmiento et al. (1995) and Toggweiler et al.(1989). The new production is based on a phosphate conservation technique in the surface water in which all phosphate brought to the surface by mixing and advection is removed as new production to restore the surface boxes to the climatological values of Levitus (Najjar et al., 1992). Remineralization of organic material is parameterized using a power law relationship with depth (Martin et al., 1987). The OBM includes a simple parameterization for the effect of remineralization on inorganic carbon using fixed remineralization coefficients between carbon and nutrients, and it uses carbonate dissociation constants as described in Millero (1995). Air–sea gas fluxes are determined from the product of the partial pressure difference between air and surface ocean, and gas transfer velocity. Gas transfer velocity is related to the annual mean wind speed for each pixel using the parameterization of Wanninkhof (1992). For comparison with the empirical results we use the grid cells centered along 24°W.

The anthropogenic CO_2 simulation in the NCAR ocean model is run in a perturbation mode following Sarmiento et al. (1992). The NCAR model incorporates the Gent and McWilliams (1990) mesoscale eddy mixing parameterization and the K-profile boundary layer scheme of Large et al. (1994). The model is driven seasonally with a surface bulk flux forcing scheme (Large et al., 1997) on a nominally $2.4° \times 2.4°$ grid with 25 layers in the vertical. For the model-data compar-

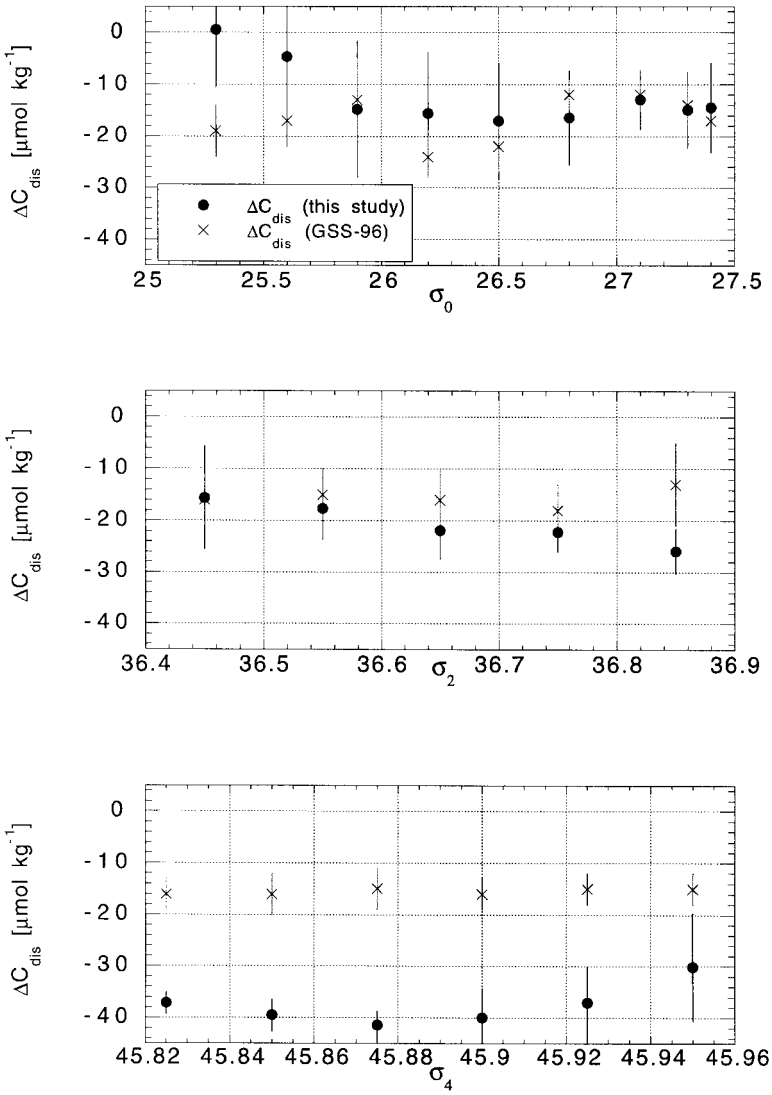

Fig. 6. Average air–water disequilibrium in terms of DIC, ΔC_{dis} for the different isopycnals (solid circles) compared to those obtained by Gruber et al. (1996) (crosses) from a different dataset. Good correspondence is observed except for the deepest water.

isons, the NCAR model is sub-sampled along 22.4°W longitude.

In the model runs, the steady state is perturbed using atmospheric CO_2 increase since 1750 from a record determined from the Siple ice core and the Mauna Loa atmospheric CO_2 record (Neftel et al., 1985; Keeling and Whorf, 1994). The Princeton OBM results show the characteristic deep penetration of DIC_{anthro} at high northern latitudes and to a lesser extend south of 25°S (Fig. 4c). A lobe of water containing greater than 5 µmol kg^{-1} DIC_{anthro} is centered near 2000 m just south of the Equator suggesting more recently ventilated water at this depth. The NCAR model results are similar (Fig. 4d). It shows slightly deeper penetration in the subtropical and tropical gyres. There is an elevated DIC_{anthro} (greater than 5 µmol/kg) in the southern tropical/subtropical

gyre at 2000 m as in the Princeton OBM but the maximum is slightly further to the north. Specific inventories along the line are very similar for the two numerical models (Fig. 5). It is not clear if the small differences are caused by different physics (e.g. mixing schemes) or resolution.

3.4. *Intercomparison of model and empirical results*

The comparison of the methods reveals many encouraging similarities and some differences. The main features of large uptake at the higher latitudes and shallow penetration of the anthropogenic signal between 25°S and 20°N is evident in all methods. Both the analyses of GSS-96 and the models show elevated concentration of DIC_{anthro} at mid depth (1500–2000 m) just south of the equator. In the empirical result this likely is associated with bifurcation of the upper deep western boundary current. The models show a recirculation cell at this depth that interacts with the boundary current and acts as a ventilation pathway (Sarmiento et al., 1995). The models and the analysis according to CM-79 show a deepening of penetration in the southern part of the section while the analysis according to the GSS-96 technique shows less. Deeper ventilation is expected due to the proximity to the southern outcrop regions. The GSS-96 analysis shows elevated DIC^{G}_{anthro} at 3000–4000 m south of 25°S that could be associated with the Antarctic bottom water spreading northward. However our observations are sparse in this area and the DIC^{G}_{anthro} is based on few data points. The patterns of DIC^{G}_{anthro} will also be a function of the preformed values in the outcrop regions that are not well constrained in the south. Errors in the preformed estimates can lead to anomalous values down stream in the deep waters.

4. Diagnostics

Since the estimates of DIC_{anthro} penetration into the ocean involve several assumptions, it is useful to determine if the inventories fit within broad geochemical and tracer constraints. The constraints that we address are: the comparison of DIC_{anthro} with CFC-11 uptake; the specific inventories of DIC_{anthro} in comparison with atmospheric burdens; and estimates of remineralization quotients for isopycnal intervals. The model results are not compared since the course vertical resolution of the bins will cause artifacts.

The CFC-11 data can be used as a qualitative gauge of the pathways of penetration of DIC_{anthro} and semi-quantitatively to estimate uptake rates if we assume that τ_{CFC} is similar to the time the water has been isolated from the atmosphere. This assumption is not exact since mixing will bias the results towards anomalously young ages, while incomplete equilibration in the outcrop regions will make the τ_{CFC} greater than the water mass age (Doney et al., 1997). The water mass age is defined as the time since the water parcel has been isolated from air–sea gas exchange. A contour plot of τ_{CFC} is shown in Fig. 7, and the 0.1 pmol kg^{-1} CFC-11 isopleth, corresponding to τ_{CFC} of 30 to 35 years, is superimposed on the DIC_{anthro} contour plots in Fig. 4. Since the mechanism of penetration of CFC and CO_2 by relatively fast air–sea gas exchange and slower, predominantly isopycnal transport into the interior are roughly similar, comparison of τ_{CFC} and DIC_{anthro} levels along isopycnals can be used to determine if the patterns of DIC_{anthro} are reasonable. Overall, the pattern of young ages at the high latitudes and older ages in the central region is similar to the DIC_{anthro} profiles. The most noticeable difference is that at high northern latitude the 0.1 pmol kg^{-1} CFC-11 isopleth is below the DIC^{G}_{anthro} contour of 5 μmol kg^{-1} while the DIC^{cm}_{anthro} has penetrated significantly deeper and southward. The Princeton and NCAR OBMs show lower penetration than expected from the CFC-11 signal at high northern latitudes as well. The numerical models have a known problem with the N. Atlantic overturning cell not penetrating deep enough in the water column.

CFC-ages can also be used in a quantitative way to estimate the rate of CO_2 uptake for select isopycnals outcropping in mid-latitudes if we make some reasonable assumptions about mixing along isopycnals. An one-endmember mixing analysis is appropriate between the wintertime outcrop region of the isopycnals between 26.8 and 27.2, and 20°N based on constant salinity values along these isopycnals. Relevant data for the N. Atl-93 cruise were linearly interpolated to the 26.8, 27.0, and 27.2 isopycnals. The latitudes of wintertime outcrop of these isopycnals determined from the inflection in the salinity along the isopycnals

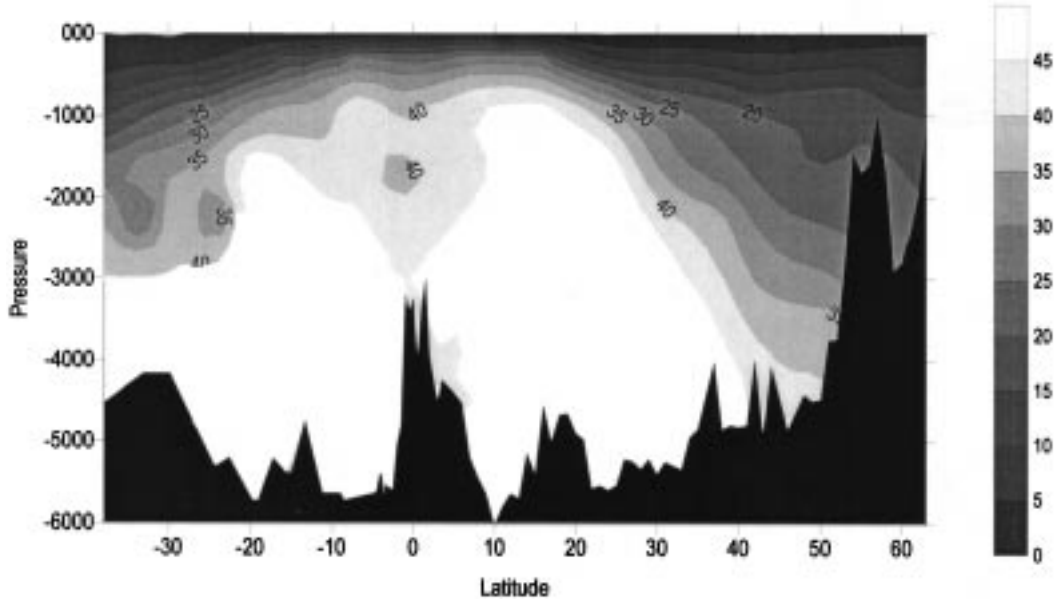

Fig. 7. Cross section of CFC-11 ages. The southern section (<5°S) are τ_{CFC} obtained from a SAVE cruise in 1989 (SAVE 5/HYDROS 4) that occupied stations along a similar transect as S. Atl-91.

(Glover and Brewer, 1988) closely correspond with the climatological outcrop areas in Levitus (1982). Assuming negligible interannual variability in uptake of CO_2 and CFCs, the slope of DIC_{anthro} versus τ_{CFC} along isopycnals should closely approximate the uptake rate. The estimated outcrop region and relevant values are shown in Table 2. Since only the change in preformed DIC is of relevance rather than the absolute DIC_{anthro} for the determination of uptake rate, the excess CO_2, CO_{2xs} was determined from:

$$DIC_{xs} = \Delta DIC - 0.5(\Delta TAlk + R_{C:N}\Delta NO_3) + R_{C:O}\Delta AOU. \quad (11)$$

The τ_{CFC} versus DIC_{xs} is shown in Fig. 8. The apparent uptake rates for 26.8, 27.0 and 27.2 are 2.0 ± 0.2, 0.9 ± 0.1, and 1.2 ± 0.1 μmol kg^{-1}yr^{-1}, respectively, where the uncertainty is the standard error in the slope of DIC_{xs} versus τ_{CFC}. For the two deeper isopycnals the uptake rate is similar to what would be expected if the upper thermoc-

Table 2. *Estimates wintertime outcrop values in N. Atlantic*

σ_t	Lat.[a)]	Depth[b)] (m)	Sal.	Temp. (°C)	CFC-11 (pM)	F-11age (yr)	CFC-12 (pmol kg^{-1})	DIC (μmol kg^{-1})	*T*Alk (μEq kg^{-1})	NO_3 (μmol kg^{-1})	AOU (μmol kg^{-1})	fCO_2 (μatm)
26.8	39	125	36.1	15.25	3.5	0	1.7	2100	2375	1.2	16	333
27	41	225	35.75	12.9	3.3	5	1.55	2123	2346	8.8	39	365
27.2	43	448	35.5	11	3.3	7	1.49	2138	2333	14.1	45	397
27.4	50	660	35.05	7.39	2.6	14	1.22	2164	2313	18	78	430

[a)] Latitude at which the salinity values show a sharp inflection along the isopycnal. The latitudes of outcropping correspond with those listed in Levitus (1982).

[b)] Depth at which inflection point occurs. All data in subsequent columns are from this depth. Values will be slightly biased compared to true outcrop values due to isolation from gas exchange and remineralization.

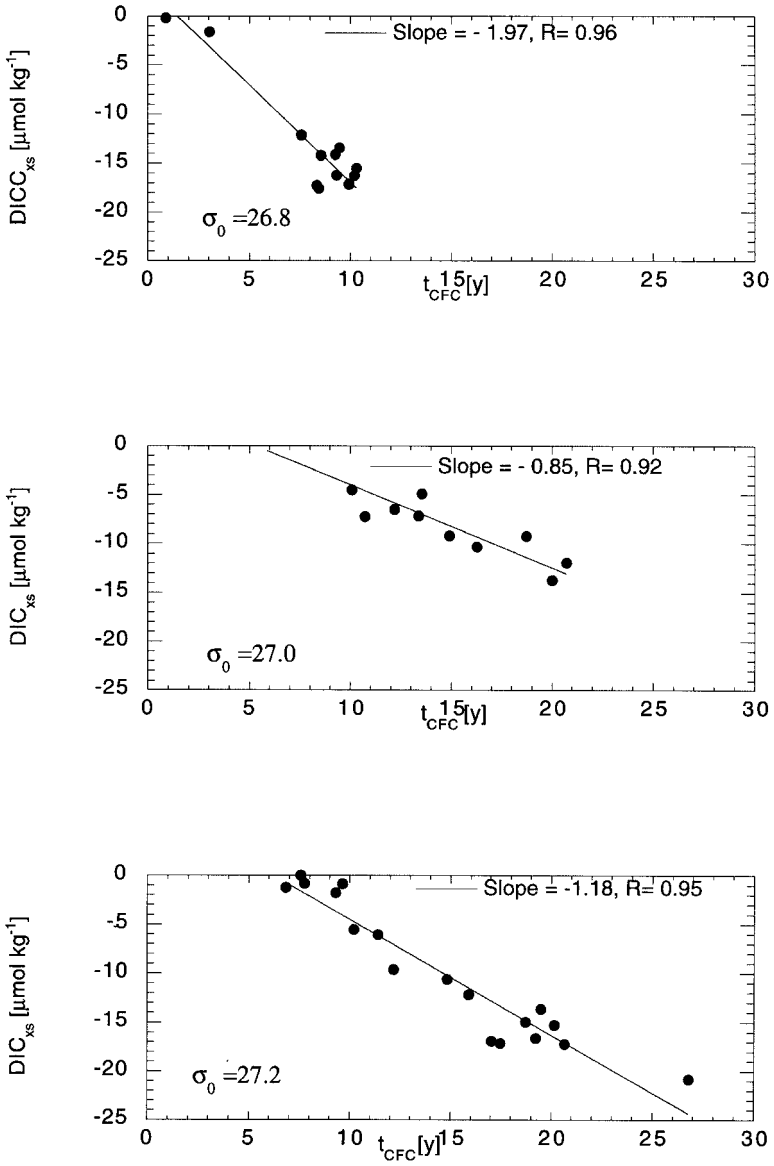

Fig. 8. Relationship between "excess DIC" referenced to the outcrop value, DIC_{xs} and τ_{CFC} for three isopycnals in the upper thermocline between 20°N and the wintertime outcrop of the particular isopycnal (Table 2). The DIC_{xs} and CFC-11 data are interpolated onto the isopycnal surfaces rather than averaging over a particular interval as done in Figs. 9, 10.

line is taking up its full burden of DIC_{anthro} with a 2 µatm increase in pCO_{2a} corresponding to 1 µmol kg^{-1}. The 26.8 isopycnal shows slightly greater uptake than would be expected, probably caused by a combination of a strong bi-modal distribution of points, centered at τ_{CFC} of 1 year and 8 years, and the difference in air–sea equilibration times for the two compounds combined with a τ_{CFC} of about a year.

The apparent uptake rate based on DIC_{xs} and τ_{CFC} has several caveats in addition to those listed above. The major one is that if the transport of

CFCs and DIC_{anthro} into the interior is not a simple pipe flow as suggested here but a combination of advection, diffusion, and mixing with surrounding water, the physical interpretation of the τ_{CFC} becomes nebulous. Based on a simple 2-D gyre model, Doney et al. (1997) suggest that tracer ages and water mass ages correspond closely in the ventilated Eastern region of the gyre where water movement is primarily advective. In the south where diffusion becomes important, the tracer and water mass ages can deviate rapidly. The offset increases with depth and distance from the outcrop.

The DIC_{anthro} versus τ_{CFC} for the deeper isopycnals (greater than 27.4) show that the DIC_{anthro} goes to zero at τ_{CFC} of about 40 years for the GSS-96 analysis (Fig. 9). Although τ_{CFC} underestimates the water mass age for older waters, the lack of DIC_{anthro} at relatively young τ_{CFC} appears to be an anomaly in the GSS-96 analysis as applied to the N. Atl-93 dataset. Over one third of the C_{anthro} burden already was in the atmosphere 40 years ago and thus it is unlikely that there would be no significant DIC_{anthro} signal for water with τ_{CFC} of 40 years. Fig. 9 also shows that the decrease DIC^{G}_{anthro} tightly follows the increase in τ_{CFC} while DIC^{cm}_{anthro} shows significantly more scatter which is probably due to the simple mixing analysis of CM-79.

A second diagnostic test of the DIC_{anthro} values is to compare the specific column burdens of C_{anthro} in atmosphere and ocean. The difference in the preanthropogenic atmospheric values estimated at 280 ppm and the annual average in 1993 of 359 ppm translates in an increase in atmospheric column burden of approximately 29 mol m^{-2}. Accounting for the land/ocean area ratio this would be equivalent to 41 mol m^{-2} for the ocean surface. The fraction of fossil fuel CO_2 release remaining airborne is roughly 50% such that values significantly greater/lower than 41 mol m^{-2} would indicate that the oceanic specific inventory is disproportionately greater/smaller. On average, the specific inventories are 40, 41, 48, and 45 mol m^{-2} from 62°N to 38°S along the transect of investigation for the Princeton OBM, the NCAR model, CM-79 and GSS-96 analyses, respectively. The extremely high column burden in the CM-79 analysis at mid-northern latitude is also manifested in the cross section by high C_{anthro} values down to the bottom (Fig. 4a) and are considered suspect.

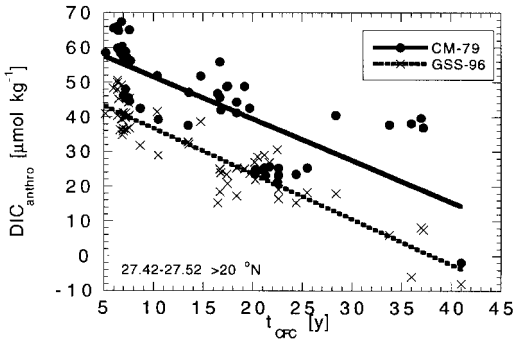

Fig. 9. Trend of DIC_{anthro} versus τ_{CFC} for empirical methods according to CM-79 and GSS-96 for the isopycnal interval between 27.42 and 27.52 north of 20°N.

The third diagnostic is to compare remineralization quotients, $R_{C:N}$ and $R_{C:O}$ along isopycnal surfaces for the measured DIC and for the preanthropogenic DIC levels, as deduced by subtracting the DIC^{G}_{anthro} or DIC^{cm}_{anthro} from the measured values. This exercise illustrates two important points. C_{anthro} has a large effect on apparent remineralization quotients when calculated from increases in inorganic carbon and nutrients along isopycnals in the thermocline. This suggests that interpretation of $R_{C:P}$, $R_{C:N}$ and $R_{C:O}$ as true remineralization coefficients should be done with caution in the upper thermocline. Secondly, the results show significant anomalies in the remineralization coefficients, particularly low $R_{C:N}$ in the N. Atlantic, that has been attributed to nitrogen fixation (Gruber and Sarmiento, 1997).

To determine the remineralization coefficients we again use the data at greater than 20°N in the thermocline to minimize the artifacts introduced by mixing northern and southern water with different preformed quantities. However, mixing artifacts could remain because of other endmembers which are present in the North Atlantic, such as the Mediterranean outflow water. The $R_{C:N}$ is computed from a least squares fit between DIC and NO_3 along isopycnals, and the resulting values are plotted versus density in Fig. 10a. The differences in $R_{C:N}$ from the measured values and the preanthropogenic values calculated according to CM-79 and GSS-96 are large, as are the differences between the two calculated preanthropogenic ratios. The $R_{C:N}$ suggested by Redfield et al. (1963), Takahashi et al. (1985), and Anderson and

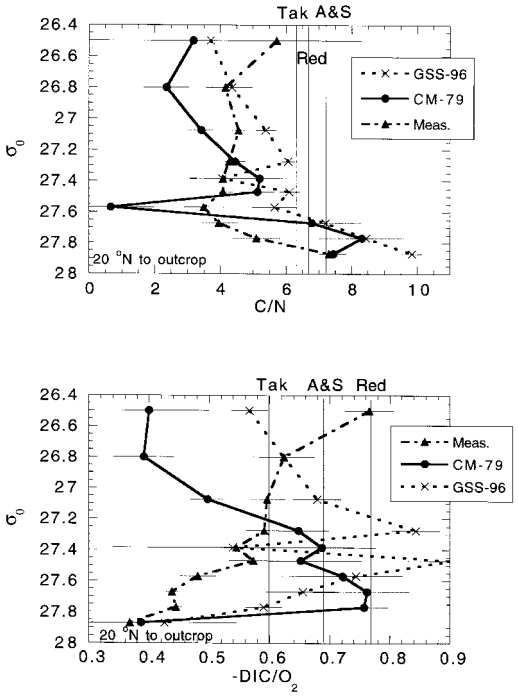

Fig. 10. Apparent remineralization quotients (Redfield ratios) versus potential density for measured DIC values (triangles and dashed lines), and for preanthropogenic DIC estimates obtained by subtracting DIC^{G}_{anthro} (crosses and dotted lines) or DIC^{cm}_{anthro} (solid circles and solid line) from the measured values. Data are from greater than 20°N to the wintertime outcrop region, or 50°N if the particular isopycnal does not outcrop. (a) The $R_{C:N}$ versus potential density interval, and (b) the $R_{C:O}$ versus potential density interval. The vertical lines are the remineralization quotients determined by Takahashi et al. (1985) (TAK); by Redfield et al. (1963) (Red); and by Anderson and Sarmiento (1994) (A&S).

Sarmiento (1994) are drawn in the figure as well for reference. Since the DIC_{anthro} is higher near the outcrop and decreases towards the interior, $R_{C:N}$ for the measured values is expected to be higher. This is not observed, except for the shallowest isopycnal (Fig. 10a). All three ratios fall below the canonical values between σ_0 of 26.8 and 27.8 because of preferential bacterial degradation of nitrogen containing organic compounds in the upper layers. This nitrate excess in the North Atlantic was also observed in the analyses of preformed nitrate by Gruber and Sarmiento (1997). Another feature is that the $R_{C:N}$ using current DIC values do not systematically fall above the corrected values using GSS-96. This is attributed to the gyre circulation with a ventilation time of about a decade (Doney et al., 1997) that causes the DIC^{G}_{anthro} to be more evenly distributed than the nitrate. The nitrate gets reset to endmember conditions every pass through the outcrop region. Thus the increase of nitrate along an isopycnal will greater than DIC^{G}_{anthro} and the $R_{C:N}$ will be lower. Based on the scatter of DIC^{cm}_{anthro} versus CFC-age (Fig. 9) we have less confidence in interpretation of the corrected $R_{C:N}$ using CM-79.

A similar exercise is performed for the $-R_{C:O}$ (Fig. 10b). The $-R_{C:O}$ shows a decreasing trend from low to high densities with the ratio changing from 0.8 to 0.4. This is consistent with a larger DIC_{anthro} gradient for the deeper isopycnals and less strong gradients above. The preanthropogenic $-R_{C:O}$ determined from GSS-96 generally fall within the accepted range of values. The $-R_{C:O}$ from the CM-79 corrected values show lower ratios throughout the water column than using GSS-96. The low $-R_{C:O}$ using the CM-79 values on the lighter isopycnals is attributed to a too high a DIC_{anthro} burden in the interior. The low $-R_{C:O}$ at σ_0 of 27.4 for the corrected DIC using GSS-96 is at similar density as the $R_{C:N}$ anomaly. This is probably caused by mixing of Mediterranean water, with lower O_2 values, towards the southern end of the area of investigation. The variations in the $-R_{C:O}$ will have a direct effect on the calculated DIC_{anthro} values since the ($R_{C:O}$ AOU) term is an important correction to DIC_{anthro} as shown in eqs. (1), (2), (7).

The trends of DIC_{anthro} with τ_{CFC}, and determination of $R_{C:N}$ and $-R_{C:O}$ offer some insights to the consistency in pattern of loading of DIC_{anthro} along the isopycnals. The DIC_{anthro} versus τ_{CFC} and the C : N analyses suggest that the penetration of DIC_{anthro} along isopycnals is shallower for the method of GSS-96 than expected from geochemical constraints. $-R_{C:O}$ and $R_{C:N}$ ratios from the CM-79 analysis show the opposite trend with high loading in the interior for the shallower isopycnal. The DIC^{cm}_{anthro} shows a lot of scatter when plotted against τ_{CFC}.

5. Conclusion

The basic principle of the two empirical methods of estimating DIC_{anthro} are similar but differ in

how preformed quantities are estimated and adjusted. The CM-79 method uses salinity normalization to correct for mixing effects of water mass, and uses subjective criteria to estimate ΔDIC_{min}. Outcrop NDIC and N*T*Alk values are assumed to be linearly correlated to temperature. The GSS-96 improves on the analyses by performing the exercise in isopycnal space and it uses a more robust parameterization of mixing effects by multiparameter linear correlations. Contamination of interior DIC by DIC_{anthro} on shallow isopycnals is corrected for in GSS-96 with transient tracers such as CFCs or $^3He/^3H$. Penetration of DIC_{anthro} in numerical models is controlled by advection and diffusion. Overall, the NCAR and Princeton models show very similar uptake patterns and uptake inventories despite different resolution and physics.

The different estimates of specific DIC_{anthro} inventories show reasonable correspondence with each other with inventories agreeing to within 20%. The inventories are in line with the oceanic sink implied from the difference in observed atmospheric CO_2 increases and fossil fuel emissions. Differences are apparent though. The estimates based on the procedures outlined in CM-79 give too high an uptake in the North Atlantic. The estimates based on GSS-96 to the contrary show the opposite effect with possibly too low a penetration in the north based on a comparison with CFC-ages. An isopycnal analysis of $R_{C:N}$, and $R_{C:O}$ using preanthropogenic DIC levels determined by subtracting the DIC_{anthro} from the measured DIC shows large variations. This suggests that simple end member mixing used in the empirical methods might not be valid. It also implies that using constant remineralization quotients to account for the remineralization at depth may introduce biases in the results. To decrease the uncertainty in future estimates of DIC_{anthro} in the ocean a variety of geochemical and empirical techniques, and models will have to be used is a synergistic manner. Anthropogenic tracers such as CFCs can be used as a diagnostic tool to assess water movement in models and as boundary conditions. Each of the methods like the empirical method and models described here has intrinsic uncertainties. However, by combining the methods and/or comparing the similarities and differences in DIC_{anthro} inventories greater confidence in the inventories can be obtained.

6. Acknowledgments

The assistance of the officers and crew of the NOAA ship *Malcolm Baldrige* is gratefully acknowledged. We wish to thank Don Atwood, and Dennis Frazel for acting as chief scientists on leg 2 of the N. Atl-93 cruise; Tom Lantry, Cathy Cosca, Hua Chen, and Dana Greeley for DIC and fCO_2 analyses; Lloyd Moore and George Berberian for nutrient analyses; David Wisegarver and Fred Menzia for CFC analyses; Gregg Thomas, Dave Bitterman, and Bob Roddy for CTD operation, and oxygen and salinity analyses; and Libby Johns for CTD data reduction. This research was funded by the NOAA Climate and Global Change (C&GC) Program. The OACES program manager, Dr. Jim Todd, is gratefully acknowledged for his support. NCAR is sponsored by the National Science Foundation. This work was supported in part by the University of Miami's Cooperative Institute for Marine and Atmospheric Studies under the National Oceanic and Atmospheric Administration's cooperative agreement NA67RJ0149.

7. Appendix A

List of symbols

AOU = apparent oxygen utilization.
DIC = total dissolved inorganic carbon.
DIC_{anthro} = anthropogenic DIC.
DIC^{cm}_{anthro} = anthropogenic DIC calculated by the method in CM-79.
DIC^{G}_{anthro} = anthropogenic DIC calculated by the method in GSS-96.
DIC_{eq} = DIC in equilibrium with a pCO_{2a} and preformed alkalinity value.
$DIC_{eq}(S, T, TAlk_0)_{pCO_{2(\tau CFC)}}$ = DIC in equilibrium with pCO_{2a} at time τ.
$DIC_{xs} = \Delta DIC - 0.5(\Delta TAlk + R_{C:N}\Delta NO_3) + R_{C:O}\Delta AOU$.
fCO_2 = fugacity of CO_2.
$NDIC_{ot}$ = current day preformed NDIC.
$NDIC_c = NDIC - 0.5[\Delta NTAlk + R_{N:O}(AOU)] + R_{C:O}AOU$.
NX = salinity normalized quantity ($= X35/S$).
pCO_{2a} = partial pressure of CO_2 in the atmosphere.
R = remineralization coefficient or "Redfield ratio".

$T\mathrm{Alk}$ = total alkalinity.
X_0 = concentration of component X in outcrop before anthropogenic perturbation. Note, $\mathrm{AOU}_0 = 0$.
X_x = concentration of species X at location x (where X = DIC, TAlk, AOU etc.).
$\Delta = X_x - X_0$.
ΔC_{dis} = difference in DIC calculated for the surface and the DIC value in equilibrium with the preanthropogenic $p\mathrm{CO}_{2\mathrm{a}}$ of 280 μatm.
$\Delta C_{\mathrm{dis_t}}$ = difference in DIC calculated for the surface and the DIC value in equilibrium with the $p\mathrm{CO}_{2\mathrm{a}}$ at time t (determined from CFC age).
$\Delta\mathrm{DIC}^{\mathrm{G}} = \mathrm{DIC} - \mathrm{DIC}_{\mathrm{eq}}(S, T, T\mathrm{Alk}_0)_{p\mathrm{CO}_{2\mathrm{a}}=280}$.
$\Delta\mathrm{DIC}^{\mathrm{cm}} = \mathrm{NDIC} - \mathrm{NDIC}_{\mathrm{ot}} - (\Delta\mathrm{NDIC})_{\mathrm{min}}$.
$\Delta\mathrm{DIC}_{\mathrm{min}} = (\mathrm{NDIC}_{\mathrm{c}} - \mathrm{NDIC}_{\mathrm{ot}})$.

REFERENCES

Anderson, L. A. and Sarmiento, J. L. 1994. Redfield ratios of remineralization determined by nutrient data analysis. *Global Biogeochem. Cycles* **8**, 65–80.

Brewer, P. G. 1978. Direct observation of the oceanic CO_2 increase. *Geophys. Res. Lett.* **5**, 997–1000.

Brewer, P. G., Wong, G. T. F., Bacon, M. P. and Spencer, D. W. 1975. An oceanic calcium problem. *Earth Planet. Sci. Lett.* **26**, 81–87.

Broecker, W. S. 1974. "NO", a conservative watermass tracer. *Earth Planet. Sci. Lett.* **23**, 100–107.

Broecker, W. S. and Ostlund, H. G. 1979. Property distributions along the sigma theta = 26.8 isopycnal in the Atlantic Ocean. *J. Geophys. Res.* **84**, 1145–1154.

Broecker, W. S., Takahashi, T. and Peng, T.-H. 1985. *Reconstruction of past atmospheric CO_2 contents from the chemistry of the contemporary ocean: an evaluation.* US Department of Energy, Washington, DC, 79 pp.

Bryan, K. and Lewis, L. J. 1979. A water mass model of the world ocean. *J. Geophys. Res.* **84**, 2503–2517.

Castle, R., Wanninkhof, R., Doney, S. C., Bullister, J., Johns, L., Feely, R. A., Huss, B. E., Millero, F. J. and Lee, K. 1998. *Chemical and hydrographic profiles and underway measurements from the North Atlantic during July and August of 1993*. NOAA data report ERL AOML-32. Springfield NJ, NOAA/AOML.

Chen, C.-T. 1993. The oceanic CO_2 sink. *Chemosphere* **27**, 1041–1064.

Chen, C.-T. and Millero, F. J. 1979. Gradual increase of oceanic CO_2. *Nature* **277**, 205–206.

Chen, C.-T. A. 1982. On the distribution of anthropogenic CO_2 in the Atlantic and Southern Oceans. *Deep-Sea Res.* **29**, 563–580.

Chen, C.-T. A., Jones, E. P. and Lin, K. 1990. Wintertime total carbon dioxide measurements in the Norwegian and Greenland Sea. *Deep-Sea Res.* **9**, 1455–1473.

Chen, H., Wanninkhof, R., Feely, R. A. and Greeley, D. 1995. *Measurement of fugacity of carbon dioxide in subsurface water: an evaluation of a method based on infrared analysis.* NOAA technical report ERL AOML-85, 52 pp. NOAA/AOML.

Chipman, D. W., Takahashi, T., Breger, D. and Sutherland, S. C. 1991. *Investigation of carbon dioxide in the South Atlantic and Northern Weddell areas (WOCE section A-12 and A-21) during the METEOR expedition 11/5 Jan.–March 1990*. Palisades, LDGO of Columbia University.

Doney, S. C. and Bullister, J. L. 1992. A chlorofluorocarbon section in the eastern North Atlantic. *Deep-Sea Res.* **39**, 1857–1883.

Doney, S. C., Jenkins, W. J. and Bullister, J. L. 1997. A comparison of ocean tracer dating techniques on a meridional section in the eastern North Atlantic. *Deep-Sea Res. I* **44**, 603–626.

Forde, E. B., Hendee, J. C. and Wanninkhof, R. 1994. *Hydrographic, carbon dioxide, nutrient, and productivity measurements from the South Atlantic during July and August of 1991*. NOAA Data Report ERL AOML-24. NOAA/AOML.

Gent, P. R. and McWilliams, J. C. 1990. Isopycnal mixing in ocean circulation models. *J. Phys. Oceanogr.* **20**, 150–155.

Glover, D. M. and Brewer, P. G. 1988. Estimates of wintertime mixed layer nutrient concentrations in the North Atlantic. *Deep-Sea Res.* **35**, 1525–1546.

Gruber, N. and Sarmiento, J. L. 1997. Global patterns of marine nitrogen fixation and denitrification. *Global Biogeochem. Cycles* **11**, 235–266.

Gruber, N., Sarmiento, J. L. and Stocker, T. F. 1996. An improved method for detecting anthropogenic CO_2 in the oceans. *Global Biogeochem. Cycles* **10**, 809–837.

Jenkins, W. J. 1988. The use of anthropogenic tritium and helium-3 to study subtropical gyre ventilation and circulation. *Phil. Trans. R. Soc. Lond. A* **325**, 43–61.

Johnson, K. M., Wills, K. D., Butler, D. B., Johnson, W. K. and Wong, C. S. 1993. Coulometric total carbon dioxide analysis for marine studies: maximizing the performance of an automated continuous gas extraction system and coulometric detector. *Mar. Chem.* **44**, 167–189.

Keeling, C. D. and Whorf, T. P. 1994. *Atmospheric CO_2 records from the sites in the SIO air sampling network.* In: T. A. Boden, D. P. Kaiser, R. J. Sepanski and F. W. Stoss (Ed.), Trends, 1993: A compendium of data on global change. Carbon Dioxide Information Analysis Center, Oak Ridge, pp. 16–24.

Körtzinger, A., Mintrop, L. and Duinker, J. C. 1998. On the penetration of anthropogenic CO_2 into the North Atlantic Ocean. *J. Geophys. Res.* **103**, 18,681–18,689.

Large, W. G., Danabasoglou, G., Doney, S. C. and McWilliams, J. C. 1997. Sensitivity to surface forcing and boundary layer mixing in a global ocean model:

annual-mean climatology. *J. Phys. Oceanogr.* **27**, 2418–2447.

Large, W. G., McWilliams, J. C. and Doney, S. C. 1994. Oceanic vertical mixing: A review and a model with a non-local boundary layer parameterization. *Rev. Geophys.* **32**, 363–403.

Lee, K., Millero, F. J. and Wanninkhof, R. 1997. The carbon dioxide system in the Atlantic Ocean. *J. Geophys. Res.* **102**, 15693–15707.

Levitus, S. 1982. *Climatological atlas of the world ocean.* Washington DC, US Government Printing Office.

Lewis, E. and Wallace, D. W. R. 1998. *Program developed for CO_2 system calculations.* Oak Ridge, ORNL/CDIAC-105, Oak Ridge National Laboratory.

Martin, J. H., Knauer, G. H., Karl, D. M. and Broenkow, W. W. 1987. VERTEX: carbon cycling in the northeast Pacific. *Deep-Sea Res.* **34**, 267–285.

Mehrbach, C., Culberson, C. H., Hawley, J. E. and Pytkowicz, R. M. 1973. Measurement of the apparent dissociation constants of carbonic acid in seawater at atmospheric pressure. *Limnol. Oceanogr.* **18**, 897–907.

Millero, F. J. 1995. Thermodynamics of the carbon dioxide system in the oceans. *Geochim. Cosmochim. Acta* **59**, 661–677.

Millero, F. J., Lee, K. and Roche, M. 1998. Distribution of alkalinity in the surface waters of the major oceans. *Mar. Chem.* **55**, 111–130.

Minster, J.-F. and Boulahdid, M. 1987. Redfield ratios along isopycnal surfaces-a complementary study. *Deep-Sea Res.* **34**, 1981–2003.

Najjar, R. G., Sarmiento, J. L. and Toggweiler, J. R. 1992. Downward transport and fate of organic matter in the ocean: Simulations with a general circulation model. *Global Biogeochem. Cycles* **6**, 45–76.

Neftel, A. E., Moor, E., Oescher, H. and Stauffer, B. 1985. Evidence from polar ice cores for the increase in atmospheric CO_2 in the past two centuries. *Nature* **315**, 45–47.

Oescher, H., Siegenthaler, U., Schotterer, U. and Gugelman, Q. 1975. A box diffusion model to study carbon dioxide exchange in nature. *Tellus* **27**, 168–192.

Redfield, A. C., Ketchum, B. H. and Richards, F. A. 1963. *The influence of organisms on the composition of seawater. In: M. N. Hill (ed.), The Sea*, vol. 2. Wiley, New York.

Sarmiento, J. L., Murnane, R. and LeQuéré, C. 1995. Air–sea CO_2 transfer and the carbon budget of the North Atlantic. *Phil. Trans. R. Soc. Lond.* **B348**, 211–219.

Sarmiento, J. L., Orr, J. C. and Siegenthaler, U. 1992. A perturbation simulation of CO_2 uptake in an ocean general circulation model. *J. Geophys. Res.* **97**, 3621–3645.

SAVE 1992. *Chemical, physical and CTD data report*. ODF-232/SIO ref 92–10. San Diego, Scripps.

Takahashi, T., Broecker, W. S. and Langer, S. 1985. Redfield ratio based on chemical data from isopycnal surfaces. *J. Geophys. Res.* **90**, 6907–6924.

Takahashi, T., Takahashi, T. T. and Sutherland, S. C. 1995. An assessment of the rôle of the North Atlantic as a CO_2 sink. *Phil. Trans. R. Soc. Lond. B* **348**, 143–152.

Takahashi, T., Weiss, R., Jenkins, W. J. and Smethie, W. M. 1994. Carbon dioxide and transient tracers in the Western Boundary Undercurrent of the North and South Atlantic ocean. *EOS, Trans. Am. Geophys. U.* **75**, 182.

Toggweiler, J. R., Dixon, K. and Bryan, K. 1989. Simulation of radiocarbon in a coarse-resolution world ocean model. 1. Steady state prebomb distributions. *J. Geophys. Res.* **94**, 8217–8242.

Tsuchiya, M., Talley, L. and McCartney, M. S. 1992. An eastern Atlantic section from Iceland southward across the equator. *Deep-Sea Res.* **39**, 1885–1917.

TTO 1986. *Transient tracers in the ocean: North Atlantic Study, shipboard physical and chemical data report*. SIO ref 86–15; PACODF no. 221, San Diego.

Wanninkhof, R. 1992. Relationship between gas exchange and wind speed over the ocean. *J. Geophys. Res.* **97**, 7373–7381.